

Thermoreversible Gel–Sol Behavior of Rod–Coil–Rod Peptide-Based Triblock Copolymers

Venkata Krishna Kotharangannagari,^{†,‡,||} Antoni Sánchez-Ferrer,^{‡,||} Janne Ruokolainen,[§] and Raffaele Mezzenga*,^{‡,†}

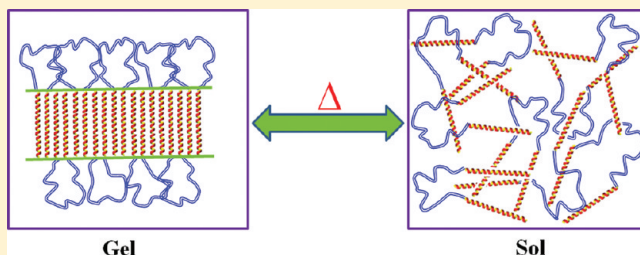
[†]Department of Physics and Frimat Center for Nanomaterials, University of Fribourg, Chemin du Musée 3, 1700 Fribourg, Switzerland

[‡]Food & Soft Materials Science, Institute of Food, Nutrition & Health, ETH Zurich, Schmelzbergstrasse 9, 8092 Zurich, Switzerland

[§]Department of Applied Physics, AALTO University, P.O. Box 15100, 00076 Helsinki, Finland

S Supporting Information

ABSTRACT: A series of peptide-based triblock copolymers consisting of poly(γ -benzyl-L-glutamate)-*b*-poly(dimethylsiloxane)-*b*-poly(γ -benzyl-L-glutamate) [PBLG-*b*-PDMS-*b*-PBLG] were synthesized using ring-opening polymerization (ROP). The chemical structure and degree of polymerizations were evaluated by ¹H NMR. These triblock copolymers form thermoreversible gels in toluene with critical gel concentration as low as 1.5 wt % and following trends which correlate directly with the secondary structure of the peptidic block. Fourier transform infrared spectroscopy (FTIR) studies indicate that the α -helical content is increased while β -sheets and random coil contents are systematically decreased with increasing volume fraction of the PBLG blocks. The gel–solution transition behavior of the triblock copolymers was examined using modulated dynamic light scattering (MDLS). It was observed that all the gels undergo gel–solution transition around 50 °C and revert back to its original state when cooling down to room temperature. Dye diffusion and diffusing wave spectroscopy (DWS) experiments showed a reduced mobility of both the dye molecules and tracer particles in the gels compared to that in solution state. The rheological studies on the organogels indicate that increasing molecular weight of the PBLG blocks or concentration of the triblock copolymers increase the gel strength considerably. Using transmission electron microscopy (TEM), the morphology of the organogels was shown to be prevalently formed by nanofibrils, with an average thickness in the range of 6–12 nm.



INTRODUCTION

The self-assembly behavior of rod–coil block copolymers is different from the common coil–coil block copolymers due to the presence of the rigid segment in their architectures and has attracted great attention in recent years.^{1–7} When dissolved in solution, in some rod–coil block copolymer systems, the polymers can form nanostructured gels in solution instead of micelles.⁸ Generally, the network formation in polymers can occur through chemical cross-linking between polymer chains or physical interactions through the entanglements or self-assembled supramolecular structures. These physical gels can exhibit reversible sol–gel transitions by changing temperature, pH, ionic strength, or concentration of the solution.⁹

Gels are a class of soft materials composed of a confined phase in a continuous three-dimensional network. On the basis of the solvent media, gels are classified in two kinds of systems: hydrogels (in aqueous medium) and organogels (in organic medium). Gels are predominantly composed of liquids; nevertheless, in terms of their mechanical response, they behave like a solid material. Moreover, in peptide-based block

copolymers, gels can be further tuned by ionic interactions, coil–coil interactions, or hydrophobic association.^{10–12}

In the case of peptide-based hydrogel systems, the gel formation is based on hydrophobic interactions due to the hydrophobicity of some amino acid residues (i.e., valine or leucine), which maintains the α -helix as a supramolecular self-assembled structure. Small peptide-based gels have been shown to undergo into molecular fibril networks and showed thermoreversibility and pH responsiveness.^{13,14} Peptide-based rod–coil diblock copolymers can form hydrogels with various potential applications in biotechnology.^{15–17}

Organogels have unique applications, which are not possible for hydrogels, and these organic-based gels are currently an area of active research.^{18–20} The peptide-based block copolymer organogel formation is similar to that of hydrogels, typically through noncovalent interactions such as hydrogen bonding,

Received: December 5, 2011

Revised: February 1, 2012

Published: February 15, 2012



$\pi-\pi$ stacking, van der Waals interactions, and solvophobic interactions.^{21–25}

Poly(γ -benzyl-L-glutamate) (PBLG) is a synthetic peptide, which forms α -helices at high degree of polymerization²⁶ by intramolecular hydrogen bonding.^{27,28} This rigid-rod-like structure of PBLG^{29–31} shows thermotropic liquid-crystalline order in bulk^{32,33} and thermoreversible gelation behavior in solution.^{34,35} Indeed, the synthesis and self-assembly of PBLG-based rod-coil block copolymers have been studied extensively due to its biocompatibility for several decades, and the resulting functional materials have several applications in the biomedical and tissue engineering field.^{36–39}

The pure PBLG homopolymer form thermoreversible gels in solvents such as toluene or benzyl alcohol passing through a lyotropic liquid-crystalline phase before gelation,^{40,41} and fibrillike network structures were found in pure PBLG homopolymer gels.³⁴ Recently, PBLG-based rod-coil diblock copolymers have been prepared, and their solutions showed thermoreversible gel formation in toluene.⁴² The mechanism for the self-assembly behavior of the PBLG-based rod-coil block copolymers suggests that a wide variety of this kind of systems with novel architectures could generate supramolecular structures in solution. Very recently, the synthesis and gel formation in toluene of PBLG-POSS (polyhedral oligomeric silsesquioxane) diblock copolymers have been reported, where the POSS block protrusion from the ribbons prevented the aggregation of the nanoribbons and allowed the formation of clear gels.⁴³ Block copolymers of poly(Z-lysine) with different coil blocks showed an increase in the gel strength with increasing the molecular weight of the peptide block.⁴⁴

Peptide-based rod-coil-rod triblock copolymers have been synthesized and studied in bulk state,^{45–48} but the thermoreversible gel-sol behavior of such systems has never been explored before. For this purpose, we synthesized and characterized a series of six rod-coil-rod triblock copolymers consisting of PBLG-*b*-PDMS-*b*-PBLG, where the degree of polymerization of the peptide-based sequences was systematically modified. The choice for these polymers (PBLG and PDMS) was based on their biocompatibility, the rigidity and self-assembly features of the PBLG block, and the low T_g and high solubility in toluene of the PDMS segment. By controlling the degree of polymerization and the α -helical content of the peptide blocks, we were able to control the self-assembly behavior of PBLG rods and the gel formation of the triblock copolymers into fibril-like networks.

EXPERIMENTAL PART

Materials. L-Glutamic acid γ -benzyl ester (Fluka, $\geq 99.0\%$), triphosgene (Aldrich, 98%), *N,N*-dimethylformamide, DMF (Sigma-Aldrich, $\geq 99.8\%$, over molecular sieve), dichloromethane, DCM (Acros, 99.99%), methanol (Fluka, 99.8%), and toluene (Fluka, $\geq 99.7\%$) were used as received. Ethyl acetate (Sigma-Aldrich, $\geq 99.9\%$) and cyclohexane (Sigma-Aldrich, $\geq 99.9\%$) were dried and distilled over CaH_2 (Fluka, $>97.0\%$) at normal pressure. Poly(dimethylsiloxane) (PDMS), diaminopropyl-terminated, was purchased from ABCR Chemicals, Germany. The (*E*)-4,4'-bis(hex-5-en-1-yloxy)azobenzene dye was synthesized accordingly to the literature.⁴⁹ Dried silica microspheres (540 nm diameter, SS03N, Bangs Laboratories) were dispersed in toluene at 10 wt % concentration.

Synthesis of (BLG-NCA) Monomer. The BLG-NCA monomer (γ -benzyl L-glutamate *N*-carboxyanhydride) was synthesized as published in our previous work.²⁶ Briefly, 15 g (63.2 mmol, 1 equiv) of γ -benzyl L-glutamate and 8.13 g (27.4 mmol, 0.43 equiv) of

triphosgene were placed in a 500 mL two-necked round-bottomed flask equipped with a magnetic stirrer, condenser, and nitrogen inlet. The system was purged with nitrogen for 10 min, 250 mL of freshly distilled ethyl acetate over CaH_2 was added, and the reaction mixture was brought to 145 °C. After several hours (5–6 h), the reactants were completely soluble, and the reaction was cooled down to room temperature. The monomer was obtained by recrystallization from ethyl acetate/cyclohexane. Yield: 15.3 g (91%). ¹H NMR (360 MHz, CDCl_3): δ = 7.10–7.42 (5H, m, Ar), 6.62 (1H, s, NH), 5.04 (2H, s, Ar-CH₂), 4.29 (1H, t, α -CH, J = 6.0 Hz), 2.50 (2H, t, γ -CH₂, J = 6.6 Hz), 2.16 (1H, m, β -CH), 2.03 (1H, m, β -CH) ppm.

Synthesis of PBLG-*b*-PDMS-*b*-PBLG Triblock Copolymers. All triblock copolymers were obtained by using the procedure described in what follows. As a representative example, the synthesis of the triblock copolymer P25 (PBLG₂₄-PDMS₃₁₄-PBLG₂₄) is described. In a 25 mL round-bottomed flask, the BLG-NCA monomer was dissolved in dry DMF under a nitrogen atmosphere. In another 10 mL round-bottomed flask, the diamino-terminated poly(dimethylsiloxane) ($\text{H}_2\text{N-PDMS-NH}_2$) macroinitiator was dissolved in dry DMF under a nitrogen atmosphere. The monomer solution was transferred to the polymer solution by syringe. The resulting mixture was stirred at room temperature for 5 days under a nitrogen atmosphere. Afterward, the solvent was removed under vacuum, and the residue was dissolved in DCM. The resulting triblock copolymer was obtained as a white solid after reprecipitation with cold methanol followed by centrifugation (3000 rpm, 0 °C). The supernatant was then removed, and this process was repeated three times. Yield: 85–90%. ¹H NMR (360 MHz, CDCl_3): δ = 9.00–7.70 (43H, NH), 7.60–6.90 (241H, Ar), 5.50–4.60 (91, Ar-CH₂), 4.50–3.60 (47H, α -CH), 2.85–1.40 (212H, β -CH₂ and γ -CH₂), 1.00–0.70 (26H, Si- β -CH₂), 0.65–0.40 (10H, Si- α -CH₂), 0.35–0.00 (1874H, Si-CH₃) ppm.

Preparation of the Organogels. The gels of PBLG-*b*-PDMS-*b*-PBLG triblock copolymers were prepared in toluene according to the published procedure.⁴² The required amounts of polymer and toluene were placed together in a sample vial. Afterward, the sealed vial was heated until the mixture became homogeneous. The polymer solution was brought to room temperature and maintained at this temperature for 48 h. Gelation was monitored—at first—by the test tube invert method. The lowest gelation concentration was identified as the critical concentration for the gelation (c_{gel}). The gel-sol transition temperature (T_{gel}) was measured by the procedure reported by Hirst et al.⁵⁰ All c_{gel} and T_{gel} values were measured in triplicates.

Techniques and Apparatus. ¹H NMR measurements were carried out at room temperature on a Bruker DPX-360 spectrometer operating at 360 MHz and using CDCl_3 as solvent.

Fourier transform infrared (FTIR) spectra of solid samples were measured at room temperature using a Bruker Tensor 27 FTIR spectrometer in attenuated total reflection (ATR) mode. For the gel samples, the FTIR measurements were performed on a Varian 640 instrument, placing the sample between two CaF_2 windows in transmission mode.

Modulated dynamic light scattering (MDLS) measurements were performed using a LS Instruments apparatus with a He-Ne laser beam (632.8 nm). The instrument is equipped with advanced modulated 3D cross-correlation technology, which suppresses the multiple scattering. Samples were prepared in glass cuvettes of 10 mm thickness. The scattered intensity fluctuations were collected at a fixed angle of 90° and averaged from three runs of 600 s each. The measurements were performed on selected samples at different temperature conditions ranging from 25 to 60 °C with 5 °C steps. Temperatures were controlled by a thermostat within an error of 0.1 °C.

Diffusing wave spectroscopy (DWS) measurements were carried out in a transmission mode using a commercial DWS apparatus (LS Instruments) with a He-Ne laser beam (λ = 632.8 nm). Samples were prepared and placed in quartz cuvettes with a 2 mm optical path length. The silica tracer nanoparticles (~20 μL) were added to the polymer solution, and the cuvette temperature was controlled with a Peltier temperature controller (± 0.2 °C), keeping the samples 10 min at the required temperature before the measurement started. The observed autocorrelation function was determined with a digital

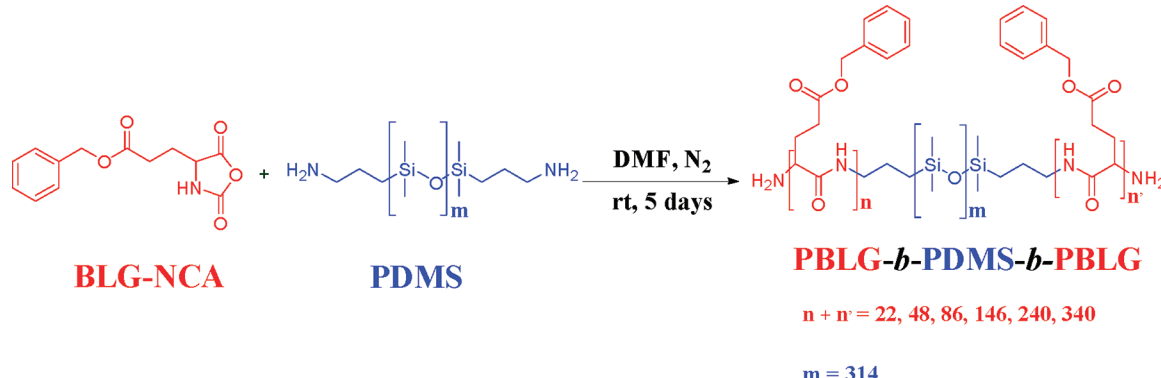
Scheme 1. Synthetic Route for the Obtaining the PBLG-*b*-PDMS-*b*-PBLG Triblock Copolymers

Table 1. Number-Average Molar Mass (M_n), Average Degree of Polymerization (DP_{PBLG}) of One PBLG Segment, Volume Fraction (ϕ_{PBLG}) of the Two PBLG Segments, Critical Gelation Concentration (c_{gel}), Gel–Sol Transition Temperature (T_{gel}), and the Theoretical Length of the Peptide Segment (L_α) in a α -Helix Conformation for the PBLG-*b*-PDMS-*b*-PBLG Triblock Copolymers

sample	block composition	M_n^a (g mol ⁻¹)	$M_{n,PBLG}^a$ (g mol ⁻¹)	DP_{PBLG}^a	ϕ_{PBLG}^b	c_{gel} (wt %)	T_{gel} (°C)	L_α^c (nm)
P13	PBLG ₁₁ -PDMS ₃₁₄ -PBLG ₁₁	27 800	4 600	11	0.13	3.5	42	1.7
P25	PBLG ₂₄ -PDMS ₃₁₄ -PBLG ₂₄	33 500	10 300	24	0.25	1.5	42	3.6
P38	PBLG ₄₃ -PDMS ₃₁₄ -PBLG ₄₃	42 000	18 800	43	0.38	1.5	44	6.5
PS1	PBLG ₇₃ -PDMS ₃₁₄ -PBLG ₇₃	55 300	32 100	73	0.51	1.5	45	11
P63	PBLG ₁₂₀ -PDMS ₃₁₄ -PBLG ₁₂₀	75 700	52 500	120	0.63	1.5	46	18
P71	PBLG ₁₇₀ -PDMS ₃₁₄ -PBLG ₁₇₀	97 800	74 600	170	0.71	1.5	46	26

^aCalculated by ¹H NMR. ^bCalculated from the following equation: $\phi_{PBLG} = M_{n,PBLG} \rho_{PBLG}^{-1} / (M_{n,PBLG} \rho_{PBLG}^{-1} + M_{n,PDMS} \rho_{PDMS}^{-1})$, where $\rho_{PBLG} = 1.278$ g cm⁻³ and $\rho_{PDMS} = 0.97$ g cm⁻³. ^cCalculated from the following equation: $L_\alpha = 0.15 DP_{PBLG}$.

correlator, and the electric field autocorrelation function $g_2(t) - 1$ was acquired over 120 s.

The mechanical properties of the organogels were studied using an AR 2000 stress-controlled rheometer (TA Instruments) with steel cone–plate configuration (20 mm diameter cone with an angle of 2°). First, a stress sweep was performed from 0.1 to 100 Pa at a frequency of 1 Hz. After a rigorous preshear (6 rad s⁻¹ in steady state, 2 min), the recovery of the gel was measured as a function of time under a stress of 0.1 Pa. Finally, a frequency sweep from 0.1 to 10 Hz was performed on the recovered gel under a stress of 0.1 Pa. The temperature of the plate was maintained at 25 °C. The gel strength was quantified by the evaluation of the shear storage modulus G' .

Transmission electron microscopy (TEM) images were acquired on a JEOL JEM-3200FSC electron microscope operating at 100 kV and bright field mode. TEM specimens were prepared by gently placing a few milligram fraction of organogel onto a carbon-coated copper grid; chemical staining to enhance phase contrast was carried out using vapors of an aqueous solution of RuO₄.

RESULTS AND DISCUSSION

In order to study the effect of the peptide volume fraction on the self-assembled gels, PBLG-*b*-PDMS-*b*-PBLG triblock copolymers were synthesized by systematically varying the PBLG content in the peptide sequence. The six different triblock copolymers with different degree of polymerization of the PBLG block were synthesized via ring-opening polymerization (ROP) of the γ -benzyl L-glutamate N-carboxyanhydride monomer (BLG-NCA)⁵¹ using the corresponding PDMS diamino-terminated polymer ($M_n = 23\,200$ g mol⁻¹) as macroinitiator according to the method described in the literature^{28,52} and shown in Scheme 1. The required amounts of monomer and macroinitiator were dissolved in DMF and under a nitrogen atmosphere. After purification, the resulting triblock copolymers were fully characterized by ¹H NMR (Supporting

Information, Figure SI-1). The degree of polymerization (DP), the average-number molecular weight (M_n), and the corresponding volume fraction of the peptide block (ϕ_{PBLG}) were evaluated by integrating the peak from the benzyl protons in the PBLG block— δ_{PBLG} (Ar—CH₂) = 5.50–4.60 ppm—and keeping the area of the peak from PDMS as constant— δ_{PDMS} (Si—CH₃) = 0.35–0.00 ppm. All the calculated values agreed with the stoichiometry used for the synthesis of the triblock copolymers and are summarized in Table 1.

For the preparation of the gels, the exact amounts of polymers and toluene were weighed in glass vials and heated to 75–80 °C for several minutes until homogeneous solutions were obtained. Afterward, the samples were brought to room temperature, and after 48 h the fully transparent gels were formed; by preparing different concentrations for each triblock copolymer, the critical gelation concentration (c_{gel}) could be determined (Table 1) and the phase diagram for the triblock copolymers constructed as shown in Figure 1. From the phase diagram, it can be observed that triblock copolymers with higher degree of polymerization can form gels at very low PBLG concentration. This trend seems to be consistent for all samples (dividing line in Figure 1) with critical gelation concentration of the triblock copolymer of 1.5 wt %. The only exception is that of the sample P13, which has very low degree of polymerization (DP = 11). As it will be shown below, this trend is the result of the very low α -helical content for this sample,²⁶ which does not promote the formation of gels. Moreover, the gel–sol transition temperature progressively increased when increasing the volume fraction of the PBLG blocks in the different samples (Supporting Information, Figure SI-2).

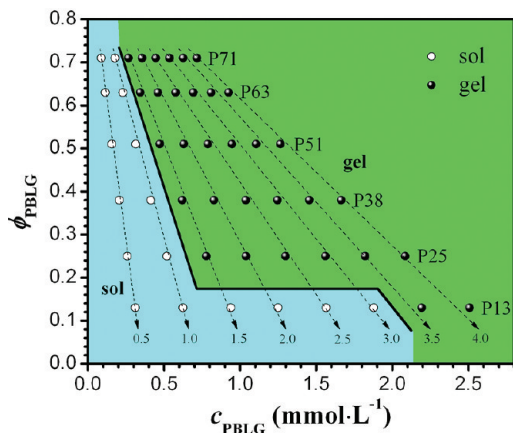


Figure 1. Phase diagram for PBLG-*b*-PDMS-*b*-PBLG triblock copolymer systems in toluene at 25 °C. (Note: the c_{PBLG} expresses the molar concentration of PBLG blocks, acting as physical linkers in the gelation process, and the numbers from the arrows are the weight percentage concentrations.)

In order to understand the influence of the secondary structure of these triblock copolymers on the gel properties, FTIR measurements were performed on all samples, both in solid state and in the gels. The FTIR spectra of all triblock copolymers in solid state clearly show characteristic absorption

peaks of the peptide secondary structures (Figure 2a). The absorption peaks at 1650–1660 cm⁻¹ (amide I) and at 1540–1550 cm⁻¹ (amide II) are characteristic of the α -helix secondary structure.⁵³ The β -sheet population has absorption peaks at 1620–1640 and 1670–1680 cm⁻¹⁵⁴ and the random coil or turn populations at 1640–1650, 1660–1670, and 1680–1690 cm⁻¹, all in the amide I region.⁵⁵ The absorbance peak at 1731 cm⁻¹ corresponds to the C=O stretching of the benzyl ester protecting group from the PBLG block. From the analysis of the amide I region and following the second derivative technique for the qualitative determination of the peaks maxima,⁵⁶ and the deconvolution technique⁵⁷ in a series of Lorentzian distributions, the populations of all secondary structures could be easily quantified⁵⁸ (Supporting Information, Figure SI-3a-d).

As shown in Figure 2a, the increase in the volume fraction of the PBLG block stabilized the α -helix content, while the β -sheet and random coil conformations decreased. The sample P13 showed mixture of α -helix and β -sheet populations, which is normal for PBLG blocks containing less than 18 residues, whereas the remaining polymers showed mainly α -helical content²⁶ with a gradual change in the secondary structure content as shown in Figure 2b. By increasing the volume fraction of the PBLG sequence, the α -helical content was increased from 56% to 89%, and the β -sheet and random coil

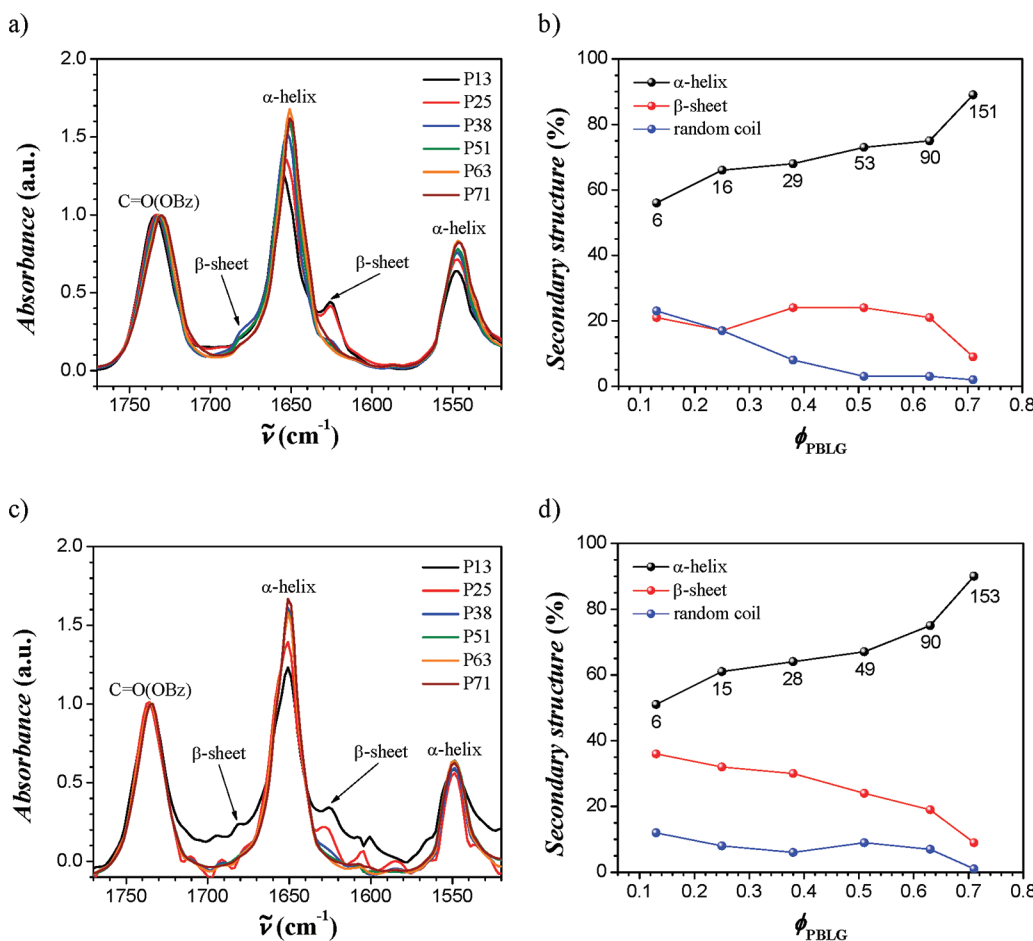


Figure 2. (a) FTIR spectra and (b) secondary structure populations for all triblock copolymers in solid state. (c) FTIR spectra and (d) secondary structure populations for all triblock copolymers in the gel state. Note: the numbers underneath black symbols are the average-number repeating units in the peptide block which contribute to the α -helical structure.

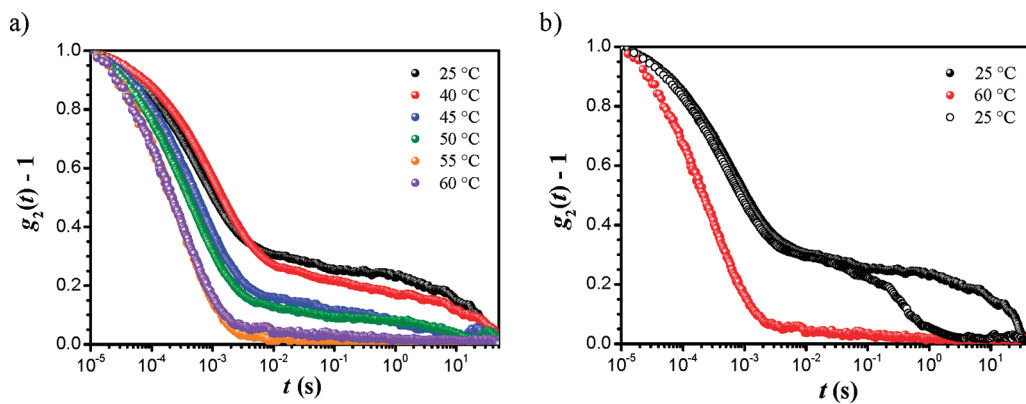


Figure 3. (a) Normalized electric field cross-correlation functions at different temperatures for the sample P63 at 2 wt % in toluene. (b) Normalized electric field cross-correlation functions at 25 °C, 60 °C, and back to 25 °C showing the thermoreversible behavior of the sample P63 at 2 wt % in toluene.

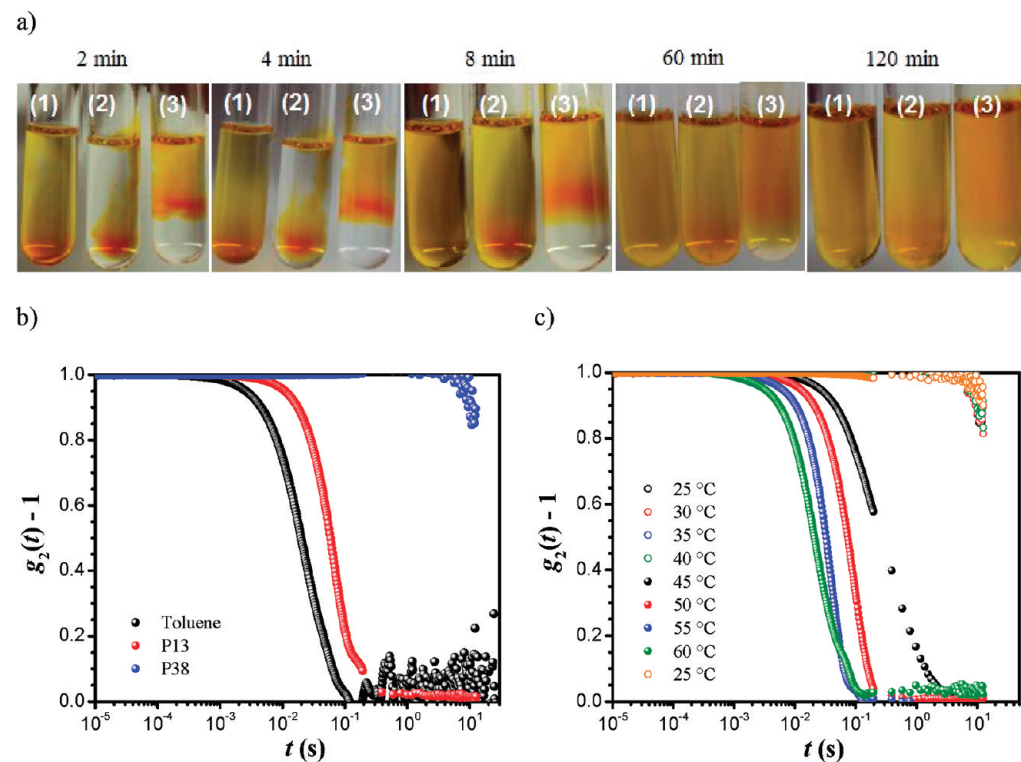


Figure 4. (a) Diffusion behavior of the azobenzene dye as a function of time in (1) toluene, (2) sample P13 at 2 wt % in toluene, and (3) sample P38 at 2 wt % in toluene at 25 °C. (b) Electric field autocorrelation function at 25 °C for the diffusion of silica tracer nanoparticles in pure toluene, in P13 and P38 at 2 wt % in toluene. (c) Electric field autocorrelation function at different temperatures for the sample P38 at 2 wt % in toluene.

populations decreased from 21% to 9% and from 23% to 2%, respectively.

Figure 2c shows the FTIR spectra of all block copolymers organogels at 25 °C and 2 wt %, with the exception of the sample P13, acquired at 4 wt %. The collected spectra agree nearly perfectly with those obtained in solid state. Thus, no significant differences were observed when the triblock copolymers formed the gel structure. In Figure 2d, the changes in α -helix population (from 51% to 90%), β -sheets (from 36% to 9%), and random coils (from 12% to 1%) as a function of the PBLG volume fraction are shown. Just small variations in the β -sheet and random coil populations can be observed, while the α -helix content remains nearly unaffected between solid and gel samples. We also run FTIR measurements at 50 °C to find out whether the gel–sol transition is originating from the

loss of secondary structure rather than changes in solubility. However, identical FTIR spectra collected at 25 °C (gel state) and at 50 °C (sol state) (Supporting Information, Figure SI-3e) allow ruling out loss of secondary structure and confirm that the gel–sol behavior arises solely from changes in solubility of the PBLG block with temperature.

In order to follow the changes during the gel–sol transition and to observe the reversibility of the systems, modulated dynamic light scattering (MDLS) experiments on the gel samples in toluene were performed. At high concentrations, multiple scattering is expected in the measurements. Thus, in order to extract the single scattering information, we make use of a MDLS setup, equipped with two detectors which cross-correlate the scattered signal from the same volume and at the same scattering vector.⁵⁹ It is well-known that the intensity and

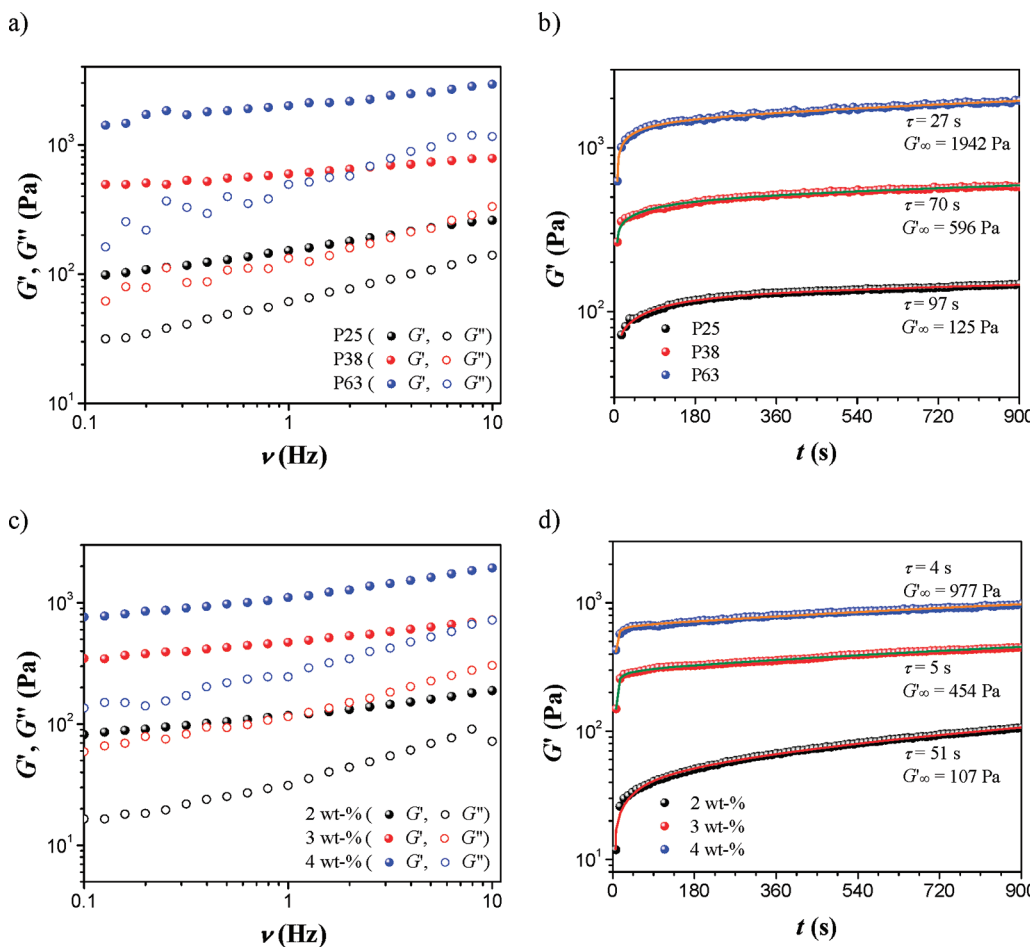


Figure 5. (a) Frequency sweeps experiments for the triblock copolymer P25, P38, and P63 at 2 wt % in toluene. (b) Recovery of the three organogels after a preshear at 6 rad s^{-1} for 2 min. (c) Frequency sweeps experiments for the triblock copolymer P38 at different concentrations in toluene. (d) Recovery after a preshear at 6 rad s^{-1} for 2 min.

electric fields correlation functions in gels decay at longer times compared to their corresponding solutions. Thus, a faster decay time should be observed when heating the gel samples above the gel–sol transition temperature. MDLS measurements were carried out on the samples P25 (PBLG₂₄-PDMS₃₁₄-PBLG₂₄), P38 (PBLG₄₃-PDMS₃₁₄-PBLG₄₃), and P63 (PBLG₁₂₀-PDMS₃₁₄-PBLG₁₂₀) at 2 wt % in the gel state from 25 to 60 °C with steps of 5 °C.

Figure 3a shows the normalized modulated electric field cross-correlation function⁶⁰ for the sample P63 at different temperatures. At 25 °C, a long relaxation decay time was observed ($\tau = 21$ s), which is common of gel-like systems, together with a second exponential decay at shorter relaxation times ($\tau = 0.6$ ms) indicative of fast molecular relaxations in the system. As soon as the temperature was gradually increased, the gel-like relaxation decay time vanished showing only one fast decay time ($\tau = 0.3$ ms). These results confirmed the presence of a gel–sol transition which was confirmed by the fluidity of the sample when the triblock copolymer was no longer self-assembled into a network.

In Figure 3b, the thermoreversible behavior of the sample P63 in the gel state when heating the sample from 25 to 60 °C and cooling back to 25 °C is shown. Again, the sample at 25 °C showed the bimodal decay time with a slow and a fast relaxation times at $\tau = 21$ s and $\tau = 0.6$ ms, respectively. After heating the sample up to 60 °C, the relaxation decay time shortened to $\tau =$

0.3 ms due to the disassembly of the network structure and the fast diffusion of the resulting macromolecules at higher temperature. When the sample was cooled down to 25 °C, the correlation function shifted back showing a bimodal decay time with higher decay times at $\tau = 0.4$ s and 0.5 ms, which indicate the thermoreversible ability of the sample to form gels. Similar behavior was also observed for the other samples P25 and P38 (Supporting Information, Figure SI-4a–d).

In order to elucidate the nature of the gels, diffusion experiments were performed at 25 °C using two different triblock copolymers (P13 and P38) at 2 wt % concentration in toluene and an azobenzene dye [(E)-4,4'-bis(hex-5-en-1-yloxy)azobenzene]. At this concentration, the two selected triblock copolymers P13 and P38 were in the solution state and in the gel state, respectively. The azobenzene dye was dropped from the top and let diffuse showing different diffusion behavior depending on the nature of the media (Figure 4a). The counter experiment with toluene alone took over 4 min to show complete diffusion of the dye, while for samples P13 and P38 diffusion was completed within 8 and 120 min, respectively. This delay in the diffusion time can be explained by the reduced mobility of the dye molecules in the presence of the triblock copolymers and strongly affected when the sample is in the gel state. These results were consistent with those from DWS experiments shown in Figure 4b. At 25 °C, the auto-correlation function for the gel-like sample P38 decayed at

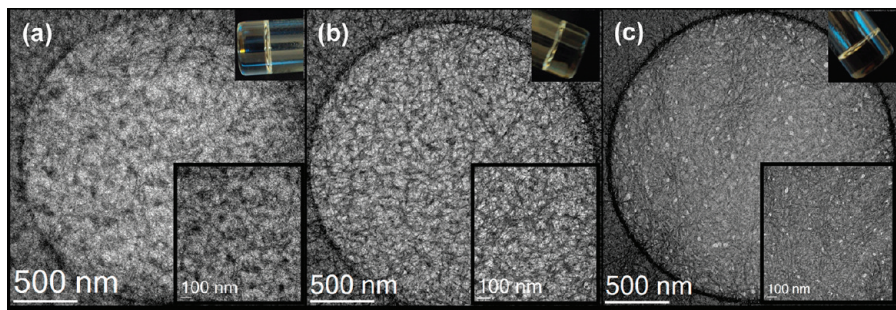


Figure 6. TEM images of the 2 wt % organogels: (a) P25, (b) P38, and (c) P63.

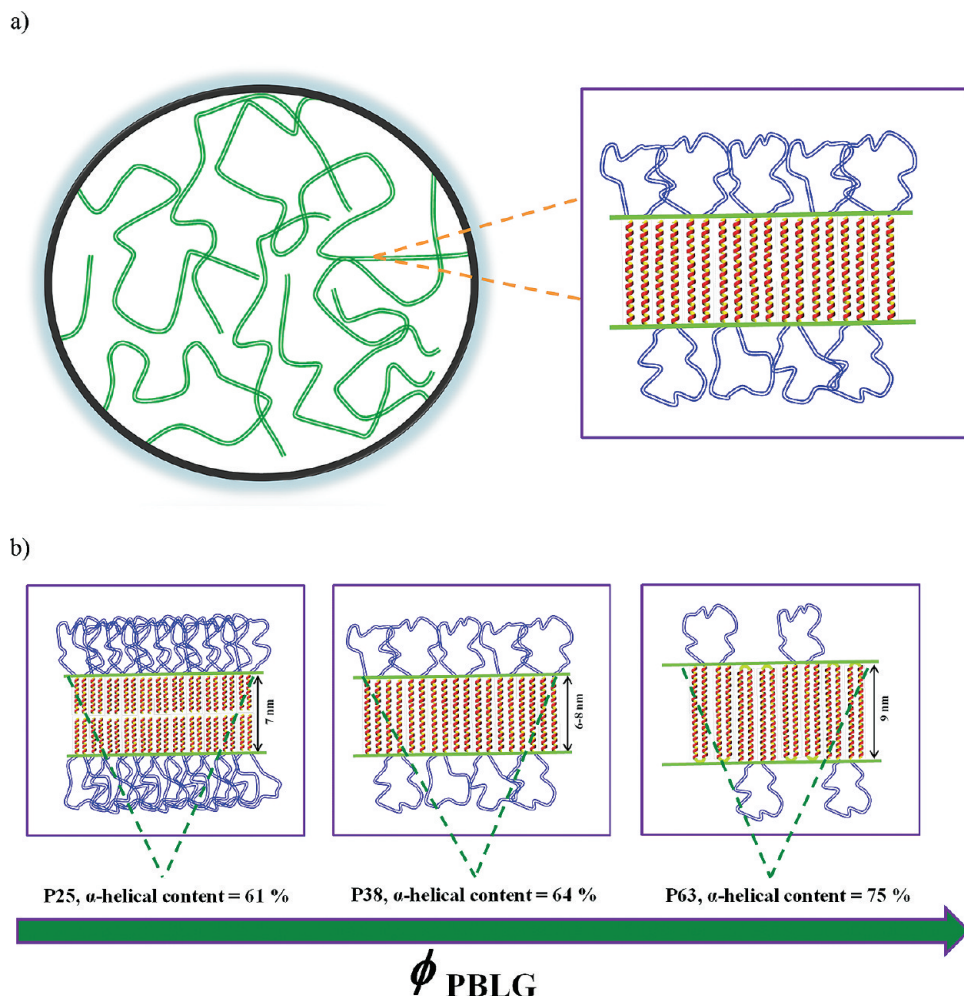


Figure 7. (a) Self-assembly of the peptide-base PBLG rods during the nanofibril formation for the PBLG-*b*-PDMS-*b*-PBLG triblock copolymers. (b) Schematic diagram for the changes in thickness due to the increase in volume fraction of the PBLG block: P25, a head-to-head morphology of the α -helical rods; P38, a monolayer morphology; and P63, a head-to-head packing of folded α -helical rods.

longer time ($\tau = 21$ s), while the sol-like sample P13 and the nanoparticles in pure toluene decayed at shorter times ($\tau = 78$ ms and $\tau = 29$ ms, respectively).

In Figure 4c, a progressive change in the correlation function as a function of temperature is shown for the sample P38. The relaxation decay time was systematically decreasing with increasing temperature from 25 °C ($\tau = 21$ s) to 60 °C ($\tau = 30$ ms) and completely restored back to 25 °C ($\tau = 21$ s). These results confirmed the presence of a reversible gel–sol transition.

Furthermore, rheology experiments were performed on the three selected samples P25, P38, and P63 in order to study the effect of the peptide's degree of polymerization of the triblock copolymers in the gel state at 2 wt %. Initially from the test tube invert method, the time required to form a gel was observed to decrease with increasing the molecular weight of the PBLG segment and concentration. Figure 5a shows the frequency sweeps with a systematic change in the shear modulus of the organogels for the three different molecular weights. At 2 wt % concentration, the storage (G') and loss (G'') moduli are directly proportional to the molecular weight of the peptide

rods. Before a preshear is applied to the samples, the storage moduli of the three gels at 1 Hz are 226, 1267, and 3042 Pa (Supporting Information, Figure SI-5a) for the samples P25, P38, and P63, respectively. When the volume fraction of the PBLG changes from $\phi_{\text{PBLG}} = 0.25$ (P25) to $\phi_{\text{PBLG}} = 0.63$ (P63), the gel strength increases more than 10 times, showing an enhancement on the mechanical properties of the material due to improved interaction between the large α -helices at $\phi_{\text{PBLG}} = 0.63$. After a preshearing at 6 rad s⁻¹ for 2 min, the time for the recovery of all organogels was also determined. Figure 5b shows the time evolution of the three gels in toluene after their complete breakdown. After 15 min, the storage moduli at 1 Hz are 125, 596, and 1942 Pa for the samples P25, P38, and P63, respectively, and their recovery times were 97, 70, and 27 s, respectively. Thus, faster restructuring of the network are observed for the high molecular weight triblock copolymers due to the ease to reform the three-dimensional structures upon increase of the peptide blocks.

Figure 5c shows the change in storage modulus for the sample P38 at three different concentrations. Initially, the storage moduli of the three gel concentrations were 423 Pa (2 wt %), 357 Pa (3 wt %), and 832 Pa (4 wt %) (Supporting Information, Figure SI-5b). This increase of the storage modulus upon increasing concentration can be explained due to increasing density of physical interactions in the network with block copolymer content, leading to stronger gels. After applying a preshear at 6 rad s⁻¹ for 2 min, the storage moduli were 107, 454, and 977 Pa for the 2, 3, and 4 wt % gel concentrations, respectively, and with recovery times of 51, 5, and 4 s. Thus, a recovery of the gel rigidity at different concentrations is observed, and at high concentration, the restructuring of the network becomes faster with block copolymer concentration (Figure 5d).

Moreover, transmission electron microscopy (TEM) experiments were performed in order to know the morphology of the self-assembled triblock copolymer organogels. The images revealed nanofibril-like morphology as shown Figure 6. After averaging the thicknesses of different nanofibrils, the widths of the corresponding self-assembled structures were found to range from 6 to 10 nm (P25), from 7 to 11 nm (P38), and from 8 to 12 nm (P63) depending on the degree of polymerization of the peptide block. These results compare reasonably well to those obtained from the calculations of the end-to-end distance of the PBLG blocks shown in Table 1.

The proposed mechanism for the establishment of these nanofibril structures is based on the microscopic phase separation of the triblock copolymers in toluene. It is well-known that the PBLG homopolymer phase separates when a homogeneous solution of this polymer is cooled down to room temperature.⁴² In the case of block copolymers where a toluene-soluble middle PDMS block is present, this microphase separation increases the local concentration of PBLG blocks and force them to self-assemble into nanofibrils. On the basis of the range of diameters of the fibrils measured, and comparing it to the length of PBLG block, one may expect the PBLG rods to align perpendicular to the long axis (in a homeotropic-like alignment) of the phase separated nanofibril domains, in the case of P25 and P38; in the case of P63, the relatively thin fibrils compared to PBLG contour length suggests possible alternative packing mechanisms (such as α -helices folding), but in all cases, the PBLG rich-nanofibrils intertwine into a 3-D network structure forming a gel.

Taking together the results of the FTIR, MDLS, rheology, and TEM analysis, the proposed mechanism for the self-assembly of the triblock copolymers in the gel state is presented in Figure 7a. All the triblock copolymers form thermoreversible organogels in toluene by the self-assembly of the rods at a concentration above their critical gelation threshold, which strongly depends on the α -helical content and the degree of polymerization of the PBLG block. The PBLG rods are confined within the core of the nanofibrils, whereas the PDMS coils remain exposed to—and swollen by—the toluene solvent molecules. Furthermore, considering the width of the fibrils, we are able to propose the packing mechanisms sketched in Figure 7b for the various triblock organogels. For the sample P25, a head-to-head morphology of the α -helix rods with 7 nm thickness is expected (homeotropic packing); for the sample P38, a monolayer morphology with 6–8 nm thickness is expected, while for the sample P63, a head-to-head packing of folded α -helix rods with 9 nm thickness is expected, in agreement with previous reports on folding of long α -helix rods.^{27,61}

CONCLUSIONS

In summary, a series of six peptide-based triblock copolymers (PBLG-*b*-PDMS-*b*-PBLG) have been synthesized using ring-opening polymerization starting from a diamino-terminated PDMS macroinitiator. These triblock copolymers form thermoreversible organogels in toluene at the critical gelation concentration of 1.5 wt %. The degree of polymerization of the PBLG block and the concentration of triblock copolymer play a key role in the gel formation and the corresponding gel strengths. The secondary structure of the resulting gels shows an increase in the α -helical content as a function of the average-number molecular weight of the rod segment. The increased volume fraction of the PBLG block results in an improved and stronger tridimensional structure of the gel. These organogels undergo gel–solution transition around 50 °C and revert back to their original state when cooling down to room temperature. The presence of gel-like and sol-like structure was studied by diffusion experiments, where the reduced mobility of an azobenzene dye molecule and silica tracer nanoparticles was observed in the gel state when compared to the solution state. The gel strength of these triblock copolymers is enhanced with increasing the molecular weight of the PBLG or the triblock copolymer concentration, leading to a denser and stronger 3D network gel. These organogels have a nanofibril-like morphology with an average thickness in the range of 6–12 nm. These results show convincingly that the structure and strength of peptide-based thermoreversible organogels can be engineered via carefully design of the molecular architecture of the block copolymer precursors.

ASSOCIATED CONTENT

S Supporting Information

¹H NMR spectra, the phase diagram showing the gel–sol transition as a function of concentration and temperature, the secondary structure evaluation from the FTIR experiments, MDLS plots, and rheological plots of the triblock copolymers. This material is available free of charge via the Internet at <http://pubs.acs.org>.

AUTHOR INFORMATION

Corresponding Author

*E-mail: raffaele.mezzenga@hest.ethz.ch.

Author Contributions

[†]The first two authors contributed equally to this study.

Notes

The authors declare no competing financial interest.

ACKNOWLEDGMENTS

The authors thank Dr. Sreenath Bolisetty, Prof. Nader Taheri, and Dr. Jani Seitsonen for the support in DLS, rheology, and TEM experiments and kind discussions. This work was carried out with the financial support of the FRIMAT center for Nanomaterials and the Swiss Science National Foundation.

REFERENCES

- (1) Lee, M.; Cho, B.; Zin, W. *Chem. Rev.* **2001**, *101*, 3869–3892.
- (2) Reenders, M.; ten Brinke, G. *Macromolecules* **2002**, *35*, 3266–3280.
- (3) Sary, N.; Mezzenga, R.; Brochon, C.; Hadzioannou, G.; Ruokolainen, J. *Macromolecules* **2007**, *40*, 3277–3286.
- (4) Sary, N.; Rubatat, L.; Brochon, C.; Hadzioannou, G.; Ruokolainen, J.; Mezzenga, R. *Macromolecules* **2007**, *40*, 6990–6997.
- (5) Sary, N.; Brochon, C.; Hadzioannou, G.; Mezzenga, R. *Eur. Phys. J. E* **2008**, *24*, 379–384.
- (6) Pryamitsyn, V.; Ganesan, V. *J. Chem. Phys.* **2004**, *120*, 5824–5838.
- (7) Jenekhe, S. A.; Chen, X. L. *Science* **1998**, *279*, 1903–1907.
- (8) Li, K.; Guo, L.; Liang, Z.; Thiagarajan, P.; Wang, Q. *J. Polym. Sci., Part A: Polym. Chem.* **2005**, *43*, 6007–6019.
- (9) Olsen, B. D.; Segalman, R. A. *Mater. Sci. Eng., R* **2008**, *62*, 37–66.
- (10) Horkay, F.; Tasaki, I.; Bassar, P. J. *Biomacromolecules* **2001**, *2*, 195–199.
- (11) Nam, K.; Watanabe, J.; Ishihara, K. *Int. J. Pharm.* **2004**, *275*, 259–269.
- (12) Qu, X.; Wirsén, A.; Albertsson, A.-C. *J. Appl. Polym. Sci.* **1999**, *74*, 3186–3192.
- (13) Pochan, D. J.; Schneider, J. P.; Kretsinger, J.; Ozbas, B.; Rajagopal, K.; Haines, L. *J. Am. Chem. Soc.* **2003**, *125*, 11802–11803.
- (14) Schneider, J. P.; Pochan, D. J.; Ozbas, B.; Rajagopal, K.; Pakstis, L.; Kretsinger, J. *J. Am. Chem. Soc.* **2002**, *124*, 15030–15037.
- (15) Breedveld, V.; Nowak, A. P.; Sato, J.; Deming, T. J.; Pine, D. J. *Macromolecules* **2004**, *37*, 3943–3953.
- (16) Nowak, A. P.; Breedveld, V.; Pakstis, L.; Ozbas, B.; Pine, D. J.; Pochan, D.; Deming, T. J. *Nature* **2002**, *417*, 424–428.
- (17) Park, M. H.; Joo, M. K.; Choi, B. G.; Jeong, B. *Acc. Chem. Res.* **2011**.
- (18) Tew, G. N.; Pralle, M. U.; Stupp, S. I. *J. Am. Chem. Soc.* **1999**, *121*, 9852–9866.
- (19) Gao, P.; Zhan, C.; Liu, L.; Zhou, Y.; Liu, M. *Chem. Commun.* **2004**, *10*, 1174–1175.
- (20) Zhan, C.; Gao, P.; Liu, M. *Chem. Commun.* **2005**, *4*, 462–464.
- (21) Markland, P.; Zhang, Y.; Amidon, G. L.; Yang, V. C. *J. Biomed. Mater. Res.* **1999**, *47*, 595–602.
- (22) Suzuki, M.; Nakajima, Y.; Yumoto, M.; Kimura, M.; Shirai, H.; Hanabusa, K. *Org. Biomol. Chem.* **2004**, *2*, 1155–1159.
- (23) Suzuki, M.; Sato, T.; Kurose, A.; Shirai, H.; Hanabusa, K. *Tetrahedron Lett.* **2005**, *46*, 2741–2745.
- (24) Terech, P.; Weiss, R. G. *Chem. Rev. (Washington, DC, U. S.)* **1997**, *97*, 3133–3159.
- (25) Van Esch, J. H.; Feringa, B. L. *Angew. Chem., Int. Ed.* **2000**, *39*, 2263–2266.
- (26) Sánchez-Ferrer, A.; Mezzenga, R. *Macromolecules* **2010**, *43*, 1093–1100.
- (27) Papadopoulos, P.; Floudas, G.; Klok, H.; Schnell, I.; Pakula, T. *Biomacromolecules* **2004**, *5*, 81–91.
- (28) Floudas, G.; Papadopoulos, P.; Klok, H.; Vandermeulen, G. W. M.; Rodriguez-Hernandez, J. *Macromolecules* **2003**, *36*, 3673–3683.
- (29) Flory, P. J. *Proc. R. Soc. London, Ser. A* **1956**, *234*, 73–89.
- (30) Uematsu, I.; Uematsu, Y. *Adv. Polym. Sci.* **1984**, *59*, 37–73.
- (31) Block, H. In *Poly(γ -benzyl-L-glutamate) and Other Glutamic Acid Containing Polymers*; Gordon and Breach Science Publishers: New York, 1983.
- (32) Robinson, C.; Ward, J. C. *Nature* **1957**, *180*, 1183–1184.
- (33) Yu, S. M.; Conticello, V. P.; Zhang, G.; Kayser, C.; Fournier, M. J.; Mason, T. L.; Tirrell, D. A. *Nature* **1997**, *389*, 167–170.
- (34) Tohyama, K.; Miller, W. G. *Nature* **1981**, *289*, 813–814.
- (35) Kuo, S. W.; Lee, H. F.; Huang, C. F.; Huang, C. J.; Chang, F. C. *J. Polym. Sci., Part A: Polym. Chem.* **2008**, *46*, 3108–3119.
- (36) Lecommandoux, S.; Achard, M.; Langenwalter, J. F.; Klok, H. *Macromolecules* **2001**, *34*, 9100–9111.
- (37) Carlsen, A.; Lecommandoux, S. *Curr. Opin. Colloid Interface Sci.* **2009**, *14*, 329–339.
- (38) Holowka, E. P.; Pochan, D. J.; Deming, T. J. *J. Am. Chem. Soc.* **2005**, *127*, 12423–12428.
- (39) Chécot, F.; Brûlet, A.; Oberdisse, J.; Gnanou, Y.; Mondain-Monval, O.; Lecommandoux, S. *Langmuir* **2005**, *21*, 4308–4315.
- (40) Doty, P.; Bradbury, J. H.; Holtzer, A. M. *J. Am. Chem. Soc.* **1956**, *78*, 947–954.
- (41) Tadmor, R.; Khalpin, R. L.; Cohen, Y. *Langmuir* **2002**, *18*, 7146–7150.
- (42) Kim, K. T.; Park, C.; Vandermeulen, G. W. M.; Rider, D. A.; Kim, C.; Winnik, M. A.; Manners, I. *Angew. Chem., Int. Ed.* **2005**, *44*, 7964–7968.
- (43) Kuo, S.; Lee, H.; Huang, W.; Jeong, K.; Chang, F. *Macromolecules* **2009**, *42*, 1619–1626.
- (44) Naik, S. S.; Savin, D. A. *Macromolecules* **2009**, *42*, 7114–7121.
- (45) Papadopoulos, P.; Floudas, G.; Schnell, I.; Lieberwirth, I.; Nguyen, T. Q.; Klok, H. *Biomacromolecules* **2006**, *7*, 618–626.
- (46) Ibarboure, E.; Rodríguez-Hernández, J.; Papon, E. *J. Polym. Sci., Part A: Polym. Chem.* **2006**, *44*, 4668–4679.
- (47) Ibarboure, E.; Papon, E.; Rodríguez-Hernández, J. *Polymer* **2007**, *48*, 3717–3725.
- (48) Ibarboure, E.; Rodríguez-Hernández, J. *Eur. Polym. J.* **2010**, *46*, 891–899.
- (49) Sánchez-Ferrer, A.; Merekalov, A.; Finkelmann, H. *Macromol. Rapid Commun.* **2011**, *32*, 672–678.
- (50) Hirst, A. R.; Smith, D. K.; Feiters, M. C.; Geurts, H. P. M.; Wright, A. C. *J. Am. Chem. Soc.* **2003**, *125*, 9010–9011.
- (51) Kotharangannagari, V. K.; Sánchez-Ferrer, A.; Ruokolainen, J.; Mezzenga, R. *Macromolecules* **2011**, *44*, 4569–4573.
- (52) Hammond, M. R.; Klok, H.; Mezzenga, R. *Macromol. Rapid Commun.* **2008**, *29*, 299–303.
- (53) Holloway, P. W.; Mantsch, H. H. *Biochemistry* **1989**, *28*, 931–935.
- (54) Dong, A.; Huang, P.; Caughey, W. S. *Biochemistry* **1990**, *29*, 3303–3308.
- (55) Surewicz, W. K.; Mantsch, H. H. *Biochim. Biophys. Acta* **1988**, *952*, 115–130.
- (56) Kauppinen, J. K.; Moffatt, D. J.; Mantsch, H. H.; Cameron, D. G. *Anal. Chem.* **1981**, *53*, 1454–1457.
- (57) Kauppinen, J. K.; Moffatt, D. J.; Mantsch, H. H.; Cameron, D. G. *Appl. Spectrosc.* **1981**, *35*, 271–276.
- (58) Yang, W. J.; Griffiths, P. R.; Byler, D. M.; Susi, H. *Appl. Spectrosc.* **1985**, *39*, 282–287.
- (59) Block, I. D.; Scheffold, F. *Rev. Sci. Instrum.* **2010**, *81*, 123107.
- (60) Park, M. J.; Char, K. *Langmuir* **2004**, *20*, 2456–2465.
- (61) Babin, J.; Taton, D.; Brinkmann, M.; Lecommandoux, S. *Macromolecules* **2008**, *41*, 1384–1392.